Cancer Chemother Pharmacol (2012) 69:397–405
DOI 10.1007/s00280-011-1706-9

ORIGINAL ARTICLE

Physiologically based pharmacokinetic modelling of high- and low-dose etoposide: from adults to children

Gisela Kersting · Stefan Willmann · Gudrun Würthwein · Jörg Lippert · Joachim Boos · Georg Hempel

Received: 9 February 2011 / Accepted: 5 July 2011 / Published online: 26 July 2011

Abstract
Purpose To evaluate the ability of a physiology-based pharmacokinetic (PBPK) model to predict the systemic drug exposure of high- and low-dose etoposide in children from a model developed with adult data.
Methods Simulations were performed with PK-Sim® (Bayer Technology Services). Model development was done using data from adult patients receiving etoposide in a conventional and high-dose polychemotherapy regimen before stem cell transplantation. Michaelis–Menten parameters from in vitro experiments reported in the literature were applied to describe the metabolism and excretion processes by P450 enzymes and transporters. The model was scaled down to children and compared to etoposide plasma concentrations in this age group.
Results Simulated plasma concentration–time courses of protein-bound and free etoposide in adults for high- and low-dose schedules agreed with the observed data. Mean simulated total clearance of high- and low-dose etoposide was 0.70 ml/min/kg ($Cl_{observed}$: 0.70 ml/min/kg) versus 0.50 ml/min/kg ($Cl_{observed}$: 0.60 ml/min/kg), respectively. Integrated Michaelis–Menten kinetics was adequately transformed to age-related pharmacokinetics in children. Predictions of the pharmacokinetics in different age groups were also in good agreement with observed data. Drug interactions triggered by *P*-glycoprotein inhibitors or nephrotoxic drugs can also be elucidated.
Conclusions The PBPK model matched the pharmacokinetics in different dosing regimens in adults. Furthermore, the scaling procedure from the adult model to children provides useful predictions for paediatric patients. Comedication with drugs influencing the metabolism and excretion has to be taken into account. This approach could be useful for planning pharmacokinetic studies in children.

Keywords Etoposide · Paediatrics · Chemotherapy · Pharmacokinetics · Modelling · Simulation

G. Kersting · G. Hempel
Department of Pharmaceutical and Medical Chemistry, Clinical Pharmacy, University of Münster, Münster, Germany

G. Kersting · J. Boos · G. Hempel
Department of Pediatric Hematology and Oncology, University Children's Hospital Münster, Münster, Germany

S. Willmann · J. Lippert
Bayer Technology Services GmbH, Competence Centre Systems Biology and Computational Solutions, 51368 Leverkusen, Germany

G. Würthwein
Centre for Clinical Trials, University of Münster, Münster, Germany

G. Hempel (✉)
Institut für Pharmazeutische und Medizinische Chemie—Klinische Pharmazie, Westfälische Wilhelms-Universität Münster, Hittorfstr. 58-62, 48149 Münster, Germany
e-mail: georg.hempel@uni-muenster.de

Introduction

Etoposide (VP-16) is a widely used anticancer drug with a broad range of antitumour activity. It is often combined with other cytotoxic agents such as cisplatin, cyclophosphamide, cytarabine or anthracyclines in a variety of paediatric leukaemia and solid tumours. The pharmacokinetics (PK) of etoposide are well characterised in both adults and children. In plasma, the drug is highly bound to plasma proteins. Renal elimination accounts for 5–50% of total systemic clearance, while the remaining amount is excreted

through the bile either unchanged or as metabolites. Some studies indicate that potential nephrotoxic drugs may affect etoposide pharmacokinetics [1]. Little is known about drug–drug interactions occurring in polychemotherapy regimens and with drugs administered for supportive care. Interactions concerning responsible metabolising enzymes and drug transporter activities consequently affect the pharmacokinetics of etoposide and may influence its efficacy or toxicity. The relationship between the pharmacokinetics and the pharmacodynamics (PD) of etoposide is well documented [2]. Developments in population software using bayesian methodology with limited sampling strategies allow the investigator to estimate PK parameters with good precision [3]. However, only few published PK–PD investigations are available referring to polychemotherapy regimens estimating the relationship between PK parameters and individual clinical and biological outcomes.

A few investigations into the population PK in children for etoposide are available [4–9]. Different physiological and anatomical attributes in children and young adults may affect the pharmacokinetic profile [10, 11]. In order to yield the optimal therapeutic effect and to avoid toxicity, precise estimates of anticancer drugs` clearances in children are required. Therefore, approaches to predict the clearance on the basis of the known metabolism and elimination processes and clearance values in adults combined with a consideration of the altered physiology and enzymatic ontogeny in children are highly desirable. In addition, it would be desirable to predict the pharmacokinetics in individuals based on patients` characteristics like renal function, comedication etc. in order to recommend an individualised dose for each patient.

Physiologically based pharmacokinetic (PBPK) modelling attempts to predict the pharmacokinetics based on drug-related and patient-related data [12]. The PBPK approach differs from classical pharmacokinetic models, because the compartments represent actual tissue and organ spaces with their physiological volumes and blood flow rates. In the simplest PBPK model, the compartments are assumed to be homogenous, and the drug enters the compartments in arterial blood and returns to the heart in the venous blood. Elimination occurs commonly in specific organs such as the kidney and the liver, and it is commonly assumed, at least for lipophilic drugs, that the uptake of drug by the tissues is either blood flow-limited or if not, the uptake can be described by a permeability-limited model.

One of the earliest descriptions of a PBPK model was that of Teorell [13]. During the early 1960s and 1970s, Bischoff and Dedrick developed a number of PBPK models particularly for anticancer drugs [14, 15]. An important application of PBPK modelling is the prediction of drug exposure to humans from animal data [16]. Recently, the prediction of infants′ pharmacokinetics becomes important regarding the regulatory guidelines for industry that push the drug development for children in different age classifications. A special age-dependent physiology database and a model are included within the PK-Sim® software allowing predictions of the pharmacokinetics, especially for the clearance by scaling adult clearances to children of all ages [17, 18]. Up to now, PBPK modelling has been applied to children only in a few cases with regard to anticancer treatment [19].

In order to assess the predictive value of the age-dependent physiology database included in PK-Sim®, we established a whole-body physiology–based model to simulate the systemic drug exposure using data from adults of high- and low-dose etoposide. Subsequently, the predictions of the model were compared to pharmacokinetic data from children receiving etoposide. We choose etoposide as a model drug, because information available on the PK in both adults and children as well as knowledge on different routes of elimination. This enables us to assess the predictive value of the PbPK approach better than applying the method to newer drugs where the knowledge is limited.

Methods

Development of the PBPK model

PBPK simulations were carried out using PK-Sim® (vers. 4.1 Bayer Technology Services GmbH, Leverkusen, Germany) [20]. The lipophilicity of etoposide is low with an log *P* of 0.9 (Drugbank-database: experimental log *P*: 1.0 and predicted log *P*: 0.73 [21]. The unbound plasma etoposide fraction varies for high- and low-dose etoposide between 4 and 11% (mean high-dose: 8.33%; mean low-dose: 5.85%) [22].

A work flow for the paediatric PBPK simulations was previously described by Edginton et al. [18]. First, an adult pharmacokinetic profile was simulated after inputting the physicochemical compound parameters, the mean body weight, height and age of the studied group and the enzyme kinetics for the metabolism and excretion processes. Based on the compound-specific physicochemical input parameters, partition coefficients were generated using the model of Rodgers and Rowland [23–25]. When the simulated curves in adults matched the mean observed data with sufficient accuracy, simulations were performed for individual concentration–time curves using the same physicochemical input parameters. The model for high-dose etoposide was evaluated in patients receiving low-dose etoposide.

Pharmacokinetic data from adults

Raw data of the nine women with primary breast cancer scheduled for a postoperative adjuvant chemotherapy

Table 1 Patients' characteristics of adult patients receiving high- and low-dose etoposide [22]

Patient	Age (years)	Height (cm)	Weight (kg)	BSA
1	48	166	91	1.74
2	46	160	57	1.59
3	38	161	57	1.6
4	28	160	63	1.65
5	55	160	67	1.63
6	35	161	56	1.48
7	51	168	55	1.62
8	47	161	51	1.52
9	52	158	60	1.58
Median	47	161	57	1.6

protocol including four cycles of conventional-dose chemotherapy and a final course of high-dose chemotherapy in combination with autologous stem cell support were available. The pharmacokinetics in seven of these women were described previously by Busse et al. [22]. Patients' characteristics are shown in Table 1 with patients 2–7 and 9 previously described in the manuscript of Busse et al. (patients 1 and 8 were not reported in that manuscript due to incomplete sampling). All patients had normal renal and liver function. The study was approved by regional ethics committee, and written informed consent was obtained from each patient.

Chemotherapy consisted of four cycles of conventional therapy and one final course of high-dose therapy with doxorubicin 35 mg/m^2, etoposide 700 mg/m^2 and cyclophosphamide 4 g/m^2.

In brief, etoposide was administered on 3 consecutive days with absolute doses between 200 and 300 mg as 1–h infusion during conventional therapy and between 1,000 and 1,300 mg (absolute) as 3-h infusion during high-dose therapy, respectively. Doxorubicin and cyclophosphamide were coadministered on day 1 during the conventional chemotherapy. The adult model was developed using high-dose etoposide and evaluated using low-dose etoposide data. Total and unbound etoposide in plasma were measured by high-performance liquid chromatography (HPLC) with electrochemical detection [26]. Pharmacokinetic calculations were performed by non-compartmental analysis using Kinetica 4.0. Values were normalised to absolute dose of 1,000 or 200 mg for high and low dose, respectively.

Pharmacokinetic data of children receiving high-dose etoposide

Pharmacokinetic data from eighteen children (boys and girls) with normal renal and liver function and different diagnoses receiving conditioning with etoposide by i.v. injection for bone marrow transplantation were available [6]. Demographic data are shown in Table 2. The patients' treatment was based on three different treatment protocols.

Protocol 1: consisted of etoposide (40 mg/kg), busulfan (divided doses daily for 4 days, total dose: 16–20 mg/kg), cyclophosphamide (twice 60 mg/kg) and anti-lymphocyte globulin (ALG) (for 3 days, total dose: 60 mg/kg);
Protocol 2: etoposide (40 mg/kg), total body irradiation (12 Gy for 3 consecutive days) and cyclophosphamide (twice 60 mg/kg);
Protocol 3: etoposide (40 mg/kg), melphalan (for 4 days, total dose 180 mg/m^2) and carboplatin (for 3 days, total dose: 1,500 mg/m^2).

Out of 18 patients, five patients received cyclosporine A (CsA, 3–6 mg/kg, Table 2). The duration of infusion was 4 h with the number of measurements available for each patient ranging from 4 to 8 plasma concentrations. The study was approved by the regional ethics committee, and informed consent was obtained from all patients and their parents. Pharmacokinetic parameters were determined by the population pharmacokinetic software P-Pharm (version 1.5).

Simulation of metabolism and excretion processes

Metabolism and active transport processes were parameterised in the model either as first order or saturable Michaelis–Menten processes in the respective organs. Hepatic enzyme activities for CYP3A4, UGT1A1, PGP, and MRP2 were taken from the literature [27–29]. Biliary excretion by PGP transport was defined by fitting the simulation results to the literature data (K_m = 255 µM, V_{max} = 0.03 µmol/min/g [30].

Furthermore, a hypothetical influx transporter was incorporated in the final model with an enzyme activity of K_m: 500 µM and a V_{max}: 0.05 µmol/min/g tissue. K_m and V_{max} values were fitted to the observed concentrations.

Net tubular secretion transport processes of etoposide were described by the apparent Michaelis–Menten constant K_m for PGP (255 µM) and cMOAT = MRP2 (616 µM). As V_{max} values were not available, the ratio of the carrier-mediated permeability (Pc) (Pc PGP = 5.96 ± 0.41 × 10^{-6} cm/s; Pc MRP2 = 1.87 ± 0.1 × 10^{-5} cm/s) values was calculated, and the predicted concentration–time curve was fitted to the observed data (V_{max} PGP = 0.15 µmol/min/g; V_{max} MRP2 = 0.45 µmol/min/g).

Etoposide clearance prediction in children

Ontogeny factors for children were taken from the literature [10] and applied to the maximum reaction velocity in case

Table 2 Patients' characteristics and pharmacokinetic parameters of children receiving high-dose etoposide [6]

Pat.	Protocol	Comedication with cyclosporine	Age (years)	Sex	Height (cm)	Weight (kg)	$Cl_{observed}$ ml/min[a]	$Cl_{simulated}$ ml/min[b]	$Cl_{simulated}$ with comedication ml/min[c]	Mean relative deviation (MRD)
1	1	Yes	0.83	F	66	9	6.36	12.3	8.91	1.31
4	2	Yes	3.5	F	91	13	8.39	19.9	14.7	1.61
10	2		13.3	F	157	54	31.2	36.2	36.2	1.34
11	2		6.2	F	125	25	12.6	28.0	28.0	2.15
17	2	Yes	14	M	152	43.3	12.8	35.9	26.9	1.88
19	2	Yes	13.9	M	162	48.7	24.5	39.9	29.7	1.53
20	2	Yes	14	F	173	73	23.4	44.5	33.6	2.46
2	3		4.3	F	104	15.4	7.61	22.5	14.0	2.79
3	3		10	M	141	32	23.9	31.7	18.2	3.02
5	3		8.9	M	138	35	23.3	30.8	17.9	4.02
7	3		4.1	M	104	15.4	10.0	22.8	13.8	1.71
8	3		3.5	F	95	15.5	8.98	21.4	12.9	1.93
9	3		1.5	M	80	9	5.62	18.2	10.8	1.79
12	3		8.8	M	128	24	12.2	27.4	15.8	1.60
13	3		2.6	M	89	13.4	8.1	21.6	12.8	1.79
14	3		8.7	M	123	21.5	9.4	25.6	14.8	1.60
15	2		8	M	131	26	12.9	28.6	28.6	4.72
16	3		4.1	M	99	14.8	7.63	21.2	12.7	1.75

Patients 6 and 18 were not analysed due to insufficient sampling. Protocol 1: busulfan (16/20 mg/kg) + etoposide (40 mg/kg) + cyclophosphamide (2*60 mg/kg); Protocol 2: total body irradiation TBI (12 Gy) + etoposide (40 mg/kg) + cyclophosphamide (2*60 mg/kg); Protocol 3: melphalan (180 mg/m^2) + etoposide (40 mg/kg) + carboplatin (1,500 mg/^{2}); *Cl* clearance

[a] Observed clearance (Cl) values in ml/min (Wurthwein et al. [6])

[b] Simulated clearance in PKSIM

[c] Simulated clearance values in PKSIM with respect to comedication

of all Michaelis–Menten processes or to the first-order rate constants describing the metabolism and excretion processes in adults [31]. Glomerular filtration rate and the activity of the hepatic enzymes involved were adjusted according to age within the PK-Sim® scaling module. Etoposide is metabolised by CYP3A4 and UGT1A1 metabolism in the proportion of 0.7 (77% excreted as hydroxyacid in urine and bile [32]) and 0.3 (29% [33]), respectively. A predicted value for age-dependent protein binding in children was generated using the scaling method described by Edginton et al. [17]. Mean plasma unbound fraction for high- and low-dose in adults ($f_{u\ adult}$ high-dose: 8.33% and $f_{u\ adult}$ low-dose: 5.85%) and the major binding plasma protein were required as input parameter for the clearance scaling in children.

Model evaluation

The validity of the PK predictions was assessed by comparing the simulated plasma concentration profiles visually with observed data. For the concentration–time curves, a mean relative deviation (MRD) was calculated and is defined as the average distance of the observed plasma concentration values from the predicted values on a logarithmic scale. An MRD value of about two means that on average, the predicted values do not deviate more a factor of two from the observed values.

The commonly used R^2 statistic (square of the Pearson product moment correlation coefficient) was used to quantify the extent of correlation between predicted and observed parameters.

Results

Evaluation of pharmacokinetic data in adults

After implementation of Michaelis–Menten constants for metabolism and excretion, the simulated mean plasma concentration–time profiles in adults normalised to 1,000 mg for high-dose and 200 mg for low-dose etoposide agreed with the observed data of total and free etoposide. To maintain the metabolism and excretion fractions defined in the literature, a hypothetical influx transporter was incorporated in the simulation. The model reached the best fit by this assumption, and the mean simulated concentration–time

curves (total Cl_{sim} high-dose: 0.70 ml/min/kg) matched the mean predicted observed data (total Cl_{obs}: 0.70 ml/min/kg) sufficiently for high-dose etoposide and described the observed data for low-dose etoposide adequately as well (total Cl_{sim} low-dose: 0.50 ml/min/kg; total Cl_{obs} low-dose: 0.60 ml/min/kg, Figs. 1a, 2a).

The amount of unchanged etoposide recovered in the bile was reported to be less than 10% [30, 34]. Using the PGP activity from the literature, the model calculates 17% biliary excretion of unchanged etoposide. As a consequence of renal (53%) and biliary excretion (17%) of unchanged etoposide, the remaining 30% have to be metabolised. Our model predicts 26% formation of the catechol and 3% of the glucuronide, respectively. Simulated fractions are shown in Figs. 1c and 2c.

The precision of the simulated versus the observed data for mean plasma concentration–time curves of high-dose etoposide was evaluated by an average MRD of 1.12 with 95% confidence interval of 0.96–1.14. The Pearson coefficient comparing mean simulated to observed concentrations was $R^2 = 0.99$ (data not shown). For low-dose etoposide, the mean MRD was 1.36 (bias: 1.01; 95% CI: 0.82–1.26) and $R^2 = 0.91$ (data not shown).

Individual plasma concentration–time curves with height and weight for each patient normalised to 1,000 mg for high-dose protein-bound etoposide ($R^2 = 0.93$) and normalised to 200 mg for low-dose protein-bound etoposide ($R^2 = 0.70$) matched the data experimentally observed in adults (Figs. 1b, 2b). Overall, the simulated data for free etoposide described the observed data precisely except for an overweight patient (high-dose etoposide) with a too low clearance prediction for free etoposide (data not shown).

Etoposide clearance prediction in children

Ontogeny information for UGT1A1, CYP3A4, glomerular filtration and tubular excretion processes by PGP was implemented in the model [8, 9, 31]. For MRP2, no ontogeny information is currently available. Integrated Michaelis–Menten and first-order kinetics of the main metabolism and excretion pathways from adults was adequately transformed to age-related pharmacokinetics in children. The predictions of the pharmacokinetics in paediatric patients of different age for high-dose etoposide by the PBPK model were in good agreement with the observed data. Individual simulated plasma concentration–time curves of representative children within every age group are shown in Fig. 3. The fractions of renal and biliary excretion were between 52 and 56% and between 15 and 18%, respectively. The metabolised fractions were calculated to be within a range from 24 to 30% for the catechol (CYP3A4) and from 3 to 4% for the glucuronide (UGT1A1), respectively.

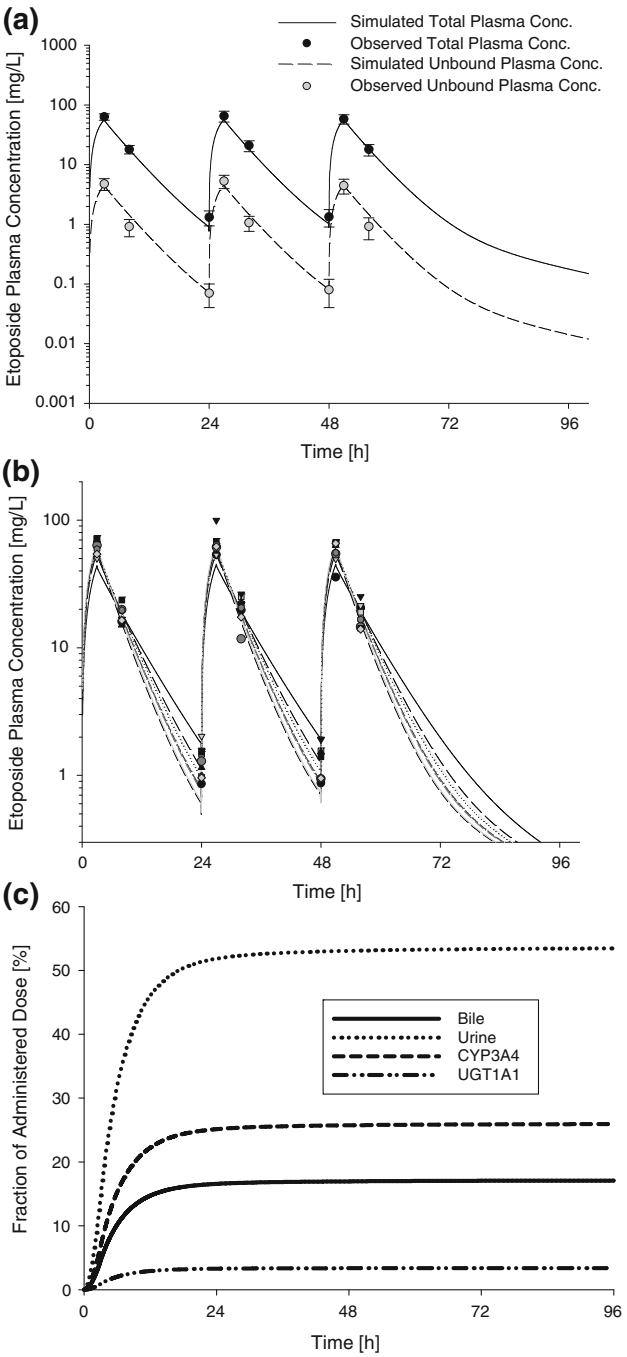

Fig. 1 High-dose etoposide simulations in adults. **a** Observed data versus mean simulated concentration–time profiles of protein-bound (*solid line*) and free (*dotted line*) etoposide. **b** Observed data from nine individuals versus simulated concentration–time profiles of protein-bound etoposide. **c** Mean fraction of administered dose excreted through bile, urine, by CYP3A4 and UGT1A1

Moreover, an influence of the coadministration of carboplatin or cyclosporine A (CsA) on the metabolism and excretion was observed. In case of carboplatin, coadministration decreased the renal clearance from an average of 53.7 to 22.4%. For individuals with carboplatin coadminis-

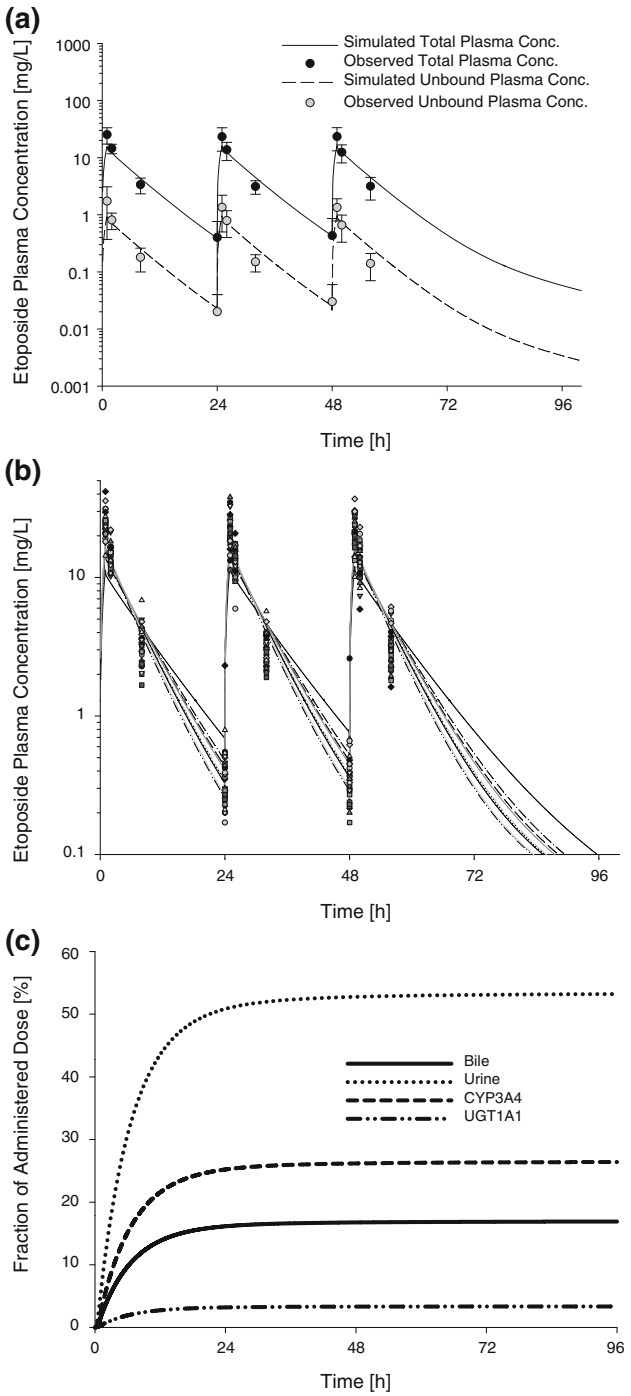

Fig. 2 Low-dose etoposide simulations in adults. **a** Observed data versus mean simulated concentration–time profiles of protein-bound (*solid line*) and free (*dotted line*) etoposide. **b** Observed data from nine individuals (four cycles each) versus simulated concentration–time profiles of protein-bound etoposide. **c** Mean fraction of administered dose excreted through bile, urine, by CYP3A4 and UGT1A1

tration, the glomerular filtration rate (GFR) and the V_{max} values of the tubular secretion transport processes (PGP and MRP2) were set to 20% of the initial value. The reduction in the total clearance by carboplatin was about 41%

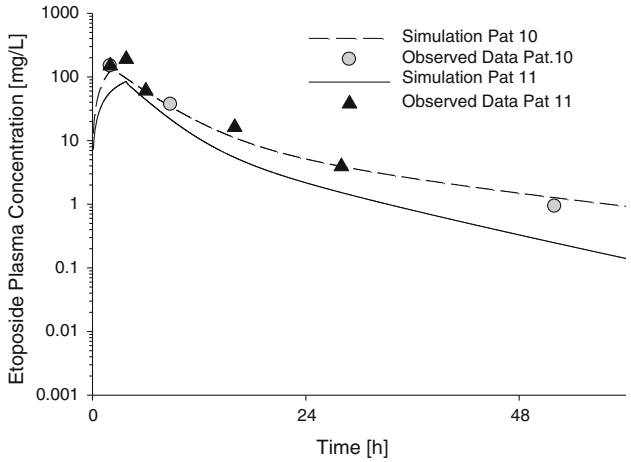

Fig. 3 Individual patient simulations after clearance scaling for etoposide in children. Individual simulated concentration–time courses of high-dose etoposide (40 mg/kg) in two representative patients; child *solid line* (*triangles*): age: 6.2 years, 125 cm, 25 kg; child *dashed line* (*points*): age: 13.3 years, 157 cm, 54 kg

(Table 2). Figure 4a shows the observed data points for a representative child versus the simulated time profile with and without the influence of carboplatin.

For CsA, V_{max} of CYP3A4 and both tubular secretion processes (PGP and MRP2) were reduced to 30 and 62% of the initial value, respectively, to reach the observed pharmacokinetic profiles by the simulation. As reported in the literature, the nonrenal clearance of etoposide via CYP3A4 was decreased by 46%. The renal clearance as seen in the excreted fractions decreased only from 53 to 49%, mainly affected by CsA on the tubular secretion transport mechanisms. V_{max} of the both tubular secretion transport processes PGP and MRP2 was reduced by 38% each**.** The total clearance decrease was 26% affected by CsA (Table 2). This effect was observed in all age groups. The influence of comedication on the simulated concentration–time curve is illustrated for a representative patient in Fig. 4b. The mean MRD of the model predictions for the 18 children was 2.17 with a 95% CI of 1.74–2.60. The higher MRD in comparison with the adult data is mainly due to patients 5 and 15 having the highest MRD values. The mean deviation of the simulated versus observed clearance was 54.1%.

Discussion

In clinical practice, paediatric dosing is done by scaling methods based on body weight or body surface area. However, these scaling methods cannot account for all physiological changes during maturation. PBPK may take these physiological changes into consideration and could finally result in a generic model applicable for all drugs, at least in those cases where all elimination pathways for the drug are

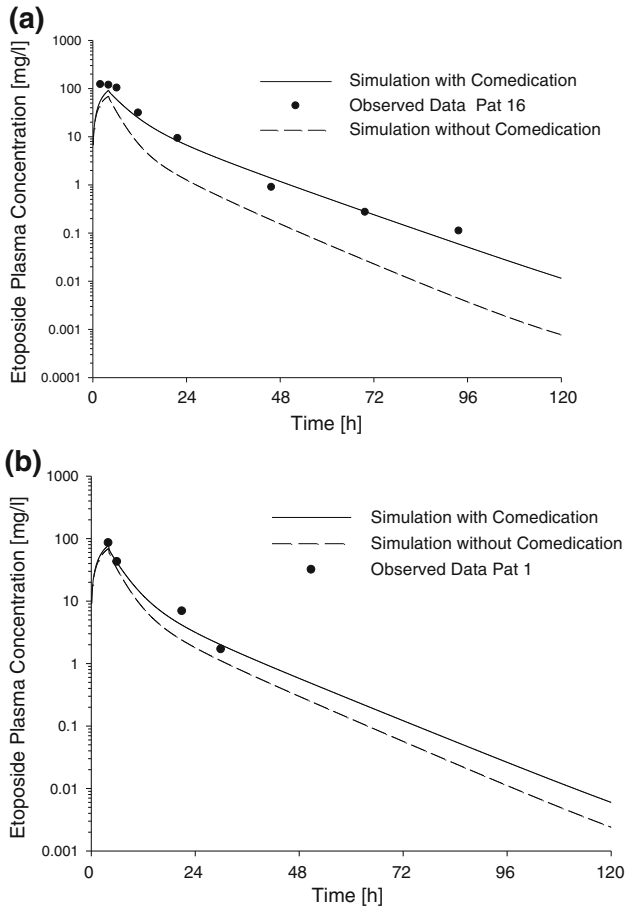

Fig. 4 Influence of coadminstration of carboplatin and cyclosporine A during high-dose polychemotherapy. **a** Observed data (*points*) for one representative child (age: 4 years, 98.8 cm, 14.8 kg) versus simulated concentration–time profile with (*solid line*) and without (*dotted line*) the influence of coadministered carboplatin 1,500 mg/m^2. **b** Observed data (*points*) for one representative child (age: 0.83 years, 66 cm, 9 kg) versus simulated concentration–time profile with (*solid line*) and without (*dotted line*) the influence of cyclosporine A (4.5–6 mg/kg iv.)

known. PBPK models have been applied to predict the exposure of children to chemicals [35–37]. By the integration of a physiological database for different age groups, PBPK allows to predict the pharmacokinetics of drugs throughout the paediatric age range.

Recently, investigations describing the capacity of different physiologically based models to predict the age dependence of clearance for various drugs were conducted [17, 38, 39]. To our knowledge, no model for etoposide or any other anticancer drugs has been reported up to date. PBPK models may provide an estimate of the pharmacokinetics of anticancer drugs in children by extrapolation of adult pharmacokinetics when no experimental pharmacokinetic data from children are available. By using PBPK models when planning studies in children, the design of these studies may be substantially improved. Using information from preclinical and clinical drug development, PBPK may help to design in vivo studies in children in order to develop a paediatric investigation plan (PIP).

In order to prove the predictive value of PBPK for anticancer drugs, a PBPK model was developed for etoposide and tested using data from an adult study. The study of Busse et al. [22] provided an excellent well-documented set of data for nine individuals as etoposide was given as monotherapy in a high-dose regimen. During conventional therapy, only a slight decrease of 10% in the clearance of etoposide due to coadministration of cyclophosphamide or doxorubicin was observed and considered to be of no clinical significance. We found this data set appropriate for our purpose, because the data are well documented and can be regarded as representative. As there are no gender effects reported for the pharmacokinetics of etoposide, the data of nine women appear sufficient to set up the model. However, model evaluation using a bigger data set from adults should be conducted.

The development of PBPK models for anticancer drugs can be difficult due to drug–drug interactions influencing the activity of metabolising enzymes or drug transporters in the multidrug therapy protocols. The application of high-dose etoposide in children included comedication with cyclosporine A (CsA) for most of the patients receiving protocol 1 or 2 (Table 2) known as an inhibitor of the PGP transporter. When etoposide was coadministered with CsA, concentrations higher than 2,000 ng/ml produced an increase in etoposide AUC of 60% [40]. In addition, Lacayo et al. [41] found that the mean clearance declined by 71% in children with CsA comedication. Therefore, the adjustment of the renal (tubular secretion) and nonrenal (CYP3A4) excretion in children with the comedication CsA in the high-dose etoposide protocol is reasonable. However, we observed a decrease of only 26% of the total clearance by CsA in this patient group.

The concomitant use of carboplatin may also change the clearance of etoposide. While Thomas et al. [42] found only a small interaction between etoposide and platinum drugs during low-dose etoposide use in adults, in another study the reduction in the clearance of high-dose etoposide in children with concurrent carboplatin was approximately 38% [43]. Thiery-Vuillemin et al. [44] found no interaction between low-dose oral etoposide and carboplatin. However, the adjustment of the simulations to the observed data for high-dose etoposide therapy in children was more precise when these considerations were taken into account. While the renal clearance was changed by carboplatin, the metabolism rate such as the formation of the catechol via CYP3A4 increased at the same time. This has to be taken into account for the use of high-dose polychemotherapy in parallel to etoposide administration.

PBPK models in general describe the tissue distribution of drugs either limited by perfusion rate (also called "well

stirred") or by permeability. The program PK-Sim® used in our PBPK model combines both models. In case of etoposide, the membrane permeability could not be fully calculated from the physicochemical properties but had to be complemented by active transport processes. Previously published PBPK models reflected the importance of PGP efflux transport as well and integrated in vitro estimated active transport rates for different tissues [45]. The pharmacokinetic parameters were estimated adequately on the basis of Michaelis–Menten kinetic constants for various metabolism and excretion processes such as renal tubular secretion (PGP and MRP2), bile excretion (PGP) and the metabolism processes by CYP3A4 and UGT1A1. The presence and location of these transporters could be confirmed in the previous investigations [27–29]. The K_m and V_{max} values for the transporters were taken from the literature for metabolism and excretion processes such as renal tubular secretion (PGP and MRP2), bile excretion (PGP) and metabolism by CYP3A4 and UGT1A1. The K_m and V_{max} values were slightly adjusted to fit the observed fractions and to the observed concentration–time values. To achieve a renal excretion of approximately 50%, a virtual influx transporter located at the apical membrane of the liver had to be implemented into the model. An investigation of Nishimura et al. regarding the intestinal permeability of etoposide in cynomolgus monkey and rats hypothesised that species differences in intestinal uptake of etoposide are associated with transport systems functionally expressed in humans and rats, but poorly expressed in monkeys [46]. This could be a hint to a yet unknown transporter involved in the distribution of etoposide.

These first results of the PBPK for etoposide may be taken as a first step to further characterise metabolism and excretion pathways and as a hypothesis searching for the expression and activity of active transporters in various tissues. Further elucidation will be gained by comparing simulation results for children receiving treatment protocols different to those in this study to assess the effect of drug–drug interactions. Taken together, pharmacokinetic predictions in children could be made by PK-Sim®, if simulations are based on adult data and scaled down to a homogenous children population with detailed information to possible influencing parameters. However, one cannot always know all important parameters for the deviations in drug clearance between patients. Yet unknown parameters may contribute to the variability in the pharmacokinetics. This could explain the deviations in clearance in patients 11, 15 and 17 (Table 2).

In the future, PBPK may be a useful tool for therapy individualisation as genetic information on enzymes and transporters as well as comedication or any other significant covariates could be used as input parameters to individualise the dose of patients, especially children.

Acknowledgments The centre for clinical trials is funded by the German Federal Office for Research and Technology (BMBF, 01KN0705). This work was supported by Bayer Technology Services GmbH.

Conflict of interest Stefan Willmann and Jörg Lippert are employees of Bayer Technology Services. Georg Hempel and Gisela Kersting received funding from Bayer Technology Services.

References

1. Palle J, Frost BM, Gustafsson G, Hellebostad M, Kanerva J, Liliemark E, Schmiegelow K, Lönnerholm G (2006) Etoposide pharmacokinetics in children treated for acute myeloid leukemia. Anticancer Drugs 17:1087–1094
2. Relling MV, McLeod HL, Bowman LC, Santana VM (1994) Etoposide pharmacokinetics and pharmacodynamics after acute and chronic exposure to cisplatin. Clin Pharmacol Ther 56:503–511
3. Panetta JC, Wilkinson M, Pui CH, Relling MV (2002) Limited and optimal sampling strategies for etoposide and etoposide catechol in children with leukaemia. J Pharmacokin Pharmacodyn 29:171–188
4. Urien S, Doz F, Giraud C, Rey E, Gentet JC, Chastagner P, Vassal G, Corradini N, Auvrignon A, Leblond P, Rubie H, Treluyer JM (2011) Developmental pharmacokinetics of etoposide in 67 children: lack of dexamethasone effect. Cancer Chemother Pharmacol 67:597–603
5. Veal GJ, Cole M, Errington J, Pearson AD, Gerrard M, Whyman G, Ellershaw C, Boddy AV (2010) Pharmacokinetics of carboplatin and etoposide in infant neuroblastoma patients. Cancer Chemother Pharmacol 65:1057–1066
6. Würthwein G, Klingebiel T, Krümpelmann S, Metz M, Schwenker K, Kranz K, Lanvers C, Boos J (2002) Population pharmacokinetics of high-dose etoposide in children receiving different conditioning regimens. Anticancer Drugs 13:101–110
7. Würthwein G, Krümpelmann S, Tillmann B, Real E, Schulze-Westhoff P, Jürgens H, Boos J (1999) Population pharmacokinetic approach to compare oral and i.v. administration of etoposide. Anticancer Drugs 10:807–814
8. Pein F, Pinkerton R, Berthaud P, Pritchard-Jones K, Dick G, Vassal G (2007) Dose finding study of oral PSC 833 combined with weekly intravenous etoposide in children with relapsed or refractory solid tumours. Eur J Cancer 43:2074–2081
9. Hijiya N, Panetta JC, Zhou Y, Kyzer EP, Howard SC, Jeha S, Razzouk BI, Ribeiro RC, Rubnitz JE, Hudson MM, Sandlund JT, Pui CH, Relling MV (2006) Body mass index does not influence pharmacokinetics or outcome of treatment in children with acute lymphoblastic leukemia. Blood 108:3997–4002
10. Kearns GL, Abdel-Rahman SM, Alander SW, Blowey DL, Leeder JS, Kauffman RE (2003) Developmental pharmacology–drug disposition, action, and therapy in infants and children. N Engl J Med 349:1157–1167
11. Haddad S, Restieri C, Krishnan K (2001) Characterization of age-related changes in body weight and organ weights from birth to adolescence in humans. J Toxicol Environ Health A 64:453–464
12. Edginton AN, Theil FP, Schmitt W, Willmann S (2008) Whole body physiologically-based pharmacokinetic models: their use in clinical drug development. Expert Opin Drug Metab Toxicol 4:1143–1152
13. Teorell T (1937) The diffusion effect upon ionic distribution: II. Experiments on ionic accumulation. Gen Physiol 21:107–122
14. Bischoff KB, Dedrick RL, Zaharko DS (1970) Preliminary model for methotrexate pharmacokinetics. J Pharm Sci 59:149–154

15. Bischoff KB, Dedrick RL, Zaharko DS, Longstreth JA (1971) Methotrexate pharmacokinetics. J Pharm Sci 60:1128–1133
16. Benowitz N, Melmon KL, Rowland M (1974) Lidocaine disposition kinetics in monkey and man. I. Prediction by a perfusion model. Clin Pharmacol Ther 16:87–98
17. Edginton AN, Schmitt W, Voith B, Willmann S (2006) A mechanistic approach for the scaling of clearance in children. Clin Pharmacokinet 45:683–704
18. Edginton AN, Schmitt W, Willmann S (2006) Development and evaluation of a generic physiologically based pharmacokinetic model for children. Clin Pharmacokinet 45:1013–1034
19. Li J, Gwilt P (2003) The effect of age on the early disposition of doxorubicin. Cancer Chemother Pharmacol 51:395–402
20. Willmann S, Lippert S, Schmitt W (2005) From physicochemistry to absorption and distribution: predictive mechanistic modelling and computational tools. Expert Opin Drug Metab Toxicol 1:159–168
21. Shah JC, Chen JR, Chow D (1989) Preformulation study of etoposide: identification of physicochemical characteristics responsible for the low and erratic oral bioavailability of etoposide. Pharm Res 6:408–412
22. Busse D, Würthwein G, Hinske C, Hempel G, Fromm MF, Eichelbaum M, Kroemer HK, Busch FW (2002) Pharmacokinetics of intravenous etoposide in patients with breast cancer: influence of dose escalation and cyclophosphamide and doxorubicin coadministration. Naunyn Schmiedebergs Arch Pharmacol 366:218–225
23. Rodgers T, Leahy D, Rowland M (2005) Physiologically based pharmacokinetic modeling 1: predicting the tissue distribution of moderate-to-strong bases. J Pharm Sci 94:1259–1276
24. Rodgers T, Rowland M (2006) Physiologically based pharmacokinetic modelling 2: predicting the tissue distribution of acids, very weak bases, neutrals and zwitterions. J Pharm Sci 95:1238–1257
25. Rodgers T, Rowland M (2007) Mechanistic approaches to volume of distribution predictions: understanding the processes. Pharm Res 24:918–933
26. Boos J, Krümpelmann S, Schulze-Westhoff P, Euting T, Berthold F, Jürgens H (1995) Steady-state levels and bone marrow toxicity of etoposide in children and infants: does etoposide require age-dependent dose calculation? J Clin Oncol 13:2954–2960
27. Kawashiro T et al (1998) A study on the metabolism of etoposide and possible interactions with antitumor or supporting agents by human liver microsomes. J Pharmacol Exp Ther 286:1294–1300
28. Watanabe Y, Nakajima M, Ohashi N, Kume T, Yokoi T (2003) Glucuronidation of etoposide in human liver microsomes is specifically catalyzed by UDP-glucuronosyltransferase 1A1. Drug Metab Dispos 31:589–595
29. Guo A, Marinaro W, Hu P, Sinko PJ (2002) Delineating the contribution of secretory transporters in the efflux of etoposide using Madin-Darby canine kidney (MDCK) cells overexpressing P-glycoprotein (Pgp), multidrug resistance-associated protein (MRP1), and canalicular multispecific organic anion transporter (cMOAT). Drug Metab Dispos 30:457–463
30. Hande KR (1992) Etoposide pharmacology. Semin Oncol 19(Suppl 13):3–9
31. Hayton WL (2000) Maturation and growth of renal function: dosing renally cleared drugs in children. AAPS PharmSci 2:E3
32. Clark PI, Slevin M (1987) The clinical pharmacology of etoposide and teniposide. Clin Pharmacokinet 12:223–252
33. Hande KR, Wolff SN, Greco FA, Hainsworth JD, Reed G, Johnson DH (1990) Etoposide kinetics in patients with obstructive jaundice. J Clin Oncol 8:1101–1107
34. Holthuis JJ (1988) Etoposide and teniposide. Bioanalysis, metabolism and clinical pharmacokinetics. Pharm Weekbl Sci 10:101–116
35. Pelekis M, Gephart LA, Lerman SE (2001) Physiological-model-based derivation of the adult and child pharmacokinetic intraspecies uncertainty factors for volatile organic compounds. Regul Toxicol Pharmacol 33:12–20
36. Price K, Haddad S, Krishnan S (2003) Physiological modeling of age-specific changes in the pharmacokinetics of organic chemicals in children. J Toxicol Environ Health A 66:417–433
37. Gentry PR, Covington TR, Clewell HJ 3rd (2003) Evaluation of the potential impact of pharmacokinetic differences on tissue dosimetry in offspring during pregnancy and lactation. Regul Toxicol Pharmacol 38:1–16
38. Bjorkman S (2005) Prediction of drug disposition in infants and children by means of physiologically based pharmacokinetic (PBPK) modelling: theophylline and midazolam as model drugs. Br J Clin Pharmacol 59:691–704
39. Ginsberg G (2004) Physiologically based pharmacokinetic (PBPK) modeling of caffeine and theophylline in neonates and adults: implications for assessing children's risks from environmental agents. J Toxicol Environ Health A 67:297–329
40. Lum BL, Kaubisch S, Yahanda AM, Adler KM, Jew L, Ehsan MN, Brophy NA, Halsey J, Gosland MP, Sikic BI (1992) Alteration of etoposide pharmacokinetics and pharmacodynamics by cyclosporine in a phase I trial to modulate multidrug resistance. J Clin Oncol 10:1635–1642
41. Lacayo NJ, Lum BL, Becton DL, Weinstein H, Ravindranath Y, Chang MN, Bomgaars L, Lauer SJ, Sikic BI, Dahl GV (2002) Pharmacokinetic interactions of cyclosporine with etoposide and mitoxantrone in children with acute myeloid leukemia. Leukemia 16:920–927
42. Thomas HD, Porter DJ, Bartelink I, Nobbs JR, Cole M, Elliott S, Newell DR, Calvert AH, Highley M, Boddy AV (2002) Randomized cross-over clinical trial to study potential pharmacokinetic interactions between cisplatin or carboplatin and etoposide. Br J Clin Pharmacol 53:83–91
43. Rodman JH (1994) Altered etoposide pharmacokinetics and time to engraftment in pediatric patients undergoing autologous bone marrow transplantation. J Clin Oncol 12:2390–2397
44. Thiery-Vuillemin A, Dobi E, Nguyen T, Royer B, Montange D, Maurina T, Kalbacher E, Bazan F, Villanueva C, Demarchi M, Chaigneau L, Ivanaj A, Pivot X (2010) Duration: escalation study of oral etoposide with carboplatin in patients with varied solid tumors. Anticancer Drugs 21:958–962
45. Fenneteau F, Turgeon J, Couture L, Michaud V, Li J, Nekka F (2009) Assessing drug distribution in tissues expressing *P*-glycoprotein through physiologically based pharmacokinetic modeling: model structure and parameters determination. Theor Biol Med Model 6:2
46. Nishimura T, Kato Y, Amano N, Ono M, Kubo Y, Kimura Y, Fujita H, Tsuji A (2008) Species difference in intestinal absorption mechanism of etoposide and digoxin between cynomolgus monkey and rat. Pharm Res 25:2467–2476